Bcl-2 Expression and p38MAPK Activity in Cells Infected with Influenza A Virus
IMPACT ON VIRALLY INDUCED APOPTOSIS AND VIRAL REPLICATION*[S]

Lucia Nencioni[‡1], Giovanna De Chiara[§1], Rossella Sgarbanti[‡], Donatella Amatore[‡], Katia Aquilano[¶], Maria E. Marcocci[‡], Annalucia Serafino[∥], Maria Torcia[**], Federico Cozzolino[**], Maria R. Ciriolo[¶‡‡], Enrico Garaci[§§], and Anna T. Palamara[‡‡¶¶2]

From the ‡Department of Public Health Sciences and ¶¶Istituto Pasteur-Fondazione Cenci Bolognetti, "Sapienza" University of Rome, 00185 Rome, the §Department of Cell Biology and Neuroscience, Istituto Superiore di Sanità, 00161 Rome, the Departments of ¶Biology and §§Experimental Medicine and Biochemical Sciences, University of Rome "Tor Vergata," 00133 Rome, the ∥Institute of Neurobiology and Molecular Medicine, Consiglio Nazionale delle Ricerche, 00133 Rome, the **Department of Clinical Physiopathology, University of Florence, 50139 Florence, and the ‡‡Scientific Institute for Research, Hospitalization, and Health Care "S. Raffaele," 00100 Rome, Italy

Previous reports have shown that various steps in the influenza A virus life cycle are impaired in cells expressing the antiapoptotic protein Bcl-2 (Bcl-2$^+$ cells). We demonstrated a direct link between Bcl-2 and the reduced nuclear export of viral ribonucleoprotein (vRNP) complexes in these cells. However, despite its negative impact on viral replication, Bcl-2 did not prevent host cells from undergoing virally triggered apoptosis. The protein's reduced antiapoptotic capacity was related to phosphorylation of its threonine 56 and serine 87 residues by virally activated p38MAPK. In infected Bcl-2$^+$ cells, activated p38MAPK was found predominantly in the cytoplasm, colocalized with Bcl-2, and both Bcl-2 phosphorylation and virally induced apoptosis were diminished by specific inhibition of p38MAPK activity. In contrast, in Bcl-2-negative (Bcl-2$^-$) cells, which are fully permissive to viral infection, p38MAPK activity was predominantly nuclear, and its inhibition decreased vRNP traffic, phosphorylation of viral nucleoprotein, and virus titers in cell supernatants, suggesting that this kinase also contributes to the regulation of vRNP export and viral replication. This could explain why in Bcl-2$^+$ cells, where p38MAPK is active in the cytoplasm, phosphorylating Bcl-2, influenza viral replication is substantially reduced, whereas apoptosis proceeds at rates similar to those observed in Bcl-2$^-$ cells. Our findings suggest that the impact of p38MAPK on the influenza virus life cycle and the apoptotic response of host cells to infection depends on whether or not the cells express Bcl-2, highlighting the possibility that the pathological effects of the virus are partly determined by the cell type it targets.

The influenza A virus, a widespread human pathogen, is characterized by a segmented negative strand RNA genome that encodes 11 viral proteins. Within the envelope, the eight viral RNA segments, associated with the nucleoprotein (NP)[3] and the polymerase complex, form helical ribonucleoprotein capsids (vRNP$_S$). After infection, the vRNP$_S$ are transported to the host cell nucleus, where they undergo transcription and replication. In the late phase of replication, newly formed RNP$_S$ are transferred from the nucleus to the cytoplasm and packaged into progeny virions (1–3). Such an essential step in the life cycle of the virus is known to be regulated in part by viral and host cell factors (4–9), including the expression of Bcl-2, which varies widely from one cell type to another (6, 10, 11). This transmembrane protein is well known for its ability to prevent the apoptotic cell death provoked by a variety of stimuli (12), a property that is markedly diminished when Bcl-2 undergoes phosphorylation by several different cellular kinases (13–16). Several lines of evidence indicate that host cell expression of Bcl-2 is associated with impaired replication of the influenza A virus (6, 17) and significant suppression of vRNP translocation into the cytoplasm (6). We have suggested that the latter effect might be related to interference of Bcl-2 with one or more cellular phosphorylation pathways, since phosphorylative events are known to play highly important roles in the regulation of vRNP traffic (5, 18, 19). One of the components of the vRNP complex, NP, is a phosphoprotein in both virions and infected cells. It has a complex network of serine and threonine residues, whose phosphorylation statuses change during the virus replication cycle (18). Interestingly, NP phosphorylation has been reported to affect export of vRNPs from the nucleus (19–21), and phosphorylated residues have been found within or near

---

[3] The abbreviations used are: NP, nucleoprotein; MAPK, mitogen-activated protein kinase; ERK, extracellular signal-regulated kinase; MEK, mitogen-activated protein kinase/extracellular signal-regulated kinase kinase; vRNP, viral ribonucleoprotein; MDCK, Madin-Darby canine kidney; FBS, fetal bovine serum; PBS, phosphate-buffered saline; DAPI, 4′,6-diamidino-2-phenylindole; Ab, antibody; PARP, poly(ADP-ribose) polymerase; MOI, multiplicity of infection; FACS, fluorescence-activated cell sorting; PI, propidium iodide; EGFP, enhanced green fluorescent protein; siRNA, small interfering RNA.

the protein's nuclear localization signal domains (reviewed in Ref. 22). Thus far, however, the specific kinases responsible for phosphorylation of vRNPs (or, more specifically, of NP) have yet to be identified (5, 19).

Influenza A virus infection is known to trigger signaling through several mitogen-activated protein kinase (MAPK) pathways in the host cell (23, 24), including the Raf/MEK/ERK cascade, which reportedly promotes vRNP traffic and virus production (5). Pleschka *et al.* (5) have shown that suppressing the activity of this pathway with the extracellular signal-regulated kinase (ERK) inhibitor U0126 significantly reduces nuclear vRNP export, and our group observed similar effects with resveratrol, a natural polyphenol that inhibits the activities of protein kinase C and its dependent c-Jun N-terminal kinase and p38MAPK pathways, without affecting the ERK cascade (7). Viral RNP phosphorylation thus appears to be mediated by several cellular kinases. In addition to its nuclear substrates, the serine threonine kinase p38MAPK also targets proteins located in the cytoplasm, including Bcl-2 (13, 25), and p38MAPK-mediated phosphorylation is one of the events capable of decreasing the antiapoptotic potential of such protein. In fact, it has been causally linked to the programmed cell death provoked by several stimuli in Bcl-2-expressing (Bcl-2$^+$) populations (13–15).

Conceivably, this interaction between p38MAPK and Bcl-2 in the cytoplasm can also have potential repercussions on p38MAPK activity within the nucleus; in a cell infected with the influenza virus, such an effect might alter several phosphorylation-dependent steps in the viral replication process, including the export of vRNPs. To test this hypothesis, we investigated the roles of Bcl-2 and p38MAPK in regulating influenza virus replication and virally induced apoptosis. We observed that infection of Bcl-2$^+$ cells was associated with lower viral replication rates, nuclear retention of the viral NP, and localization of activated p38MAPK in the cytosol, whereby it phosphorylated Bcl-2 and diminished its ability to prevent programmed cell death. Consequently, virus-induced apoptosis in these cells proceeded at the same rate observed in Bcl-2-negative (Bcl-2$^-$) cells. In the absence of the antiapoptotic protein, however, p38MAPK activity was predominantly nuclear, and it made a clear contribution to the export of vRNPs to the cytosol.

EXPERIMENTAL PROCEDURES

Cell Cultures

Madin-Darby canine kidney (MDCK) cells were grown in RPMI 1640 medium supplemented with 10% fetal bovine serum (FBS), glutamine (0.3 mg/ml), penicillin (100 units/ml), and streptomycin (100 mg/ml). Human neuroblastoma cells (SH-SY5Y) were maintained in Dulbecco's modified Eagle's medium/F-12 supplemented with 15% FBS and antibiotics. Cell viability was estimated by trypan blue (0.02%) exclusion. All reagents were purchased from Invitrogen.

Reagents

Unless otherwise stated, all commercial products mentioned hereafter were used according to the manufacturers' instructions. Annexin-V conjugated with Alexa Fluor-568 or Alexa Fluor-488 was purchased from Molecular Probes. Propidium iodide (Sigma)

was diluted to 50 μg/ml in phosphate-buffered saline (PBS). 4′,6-Diamidino-2-phenylindole (DAPI; Molecular Probes) was diluted to 1 mg/ml in PBS. Stock solutions of SB203580, SB202474, and PD98059 (Calbiochem) dissolved in DMSO were diluted in RPMI to final concentrations of 5, 10, and 20 μM. A stock solution of U0126 (Promega) dissolved in DMSO was diluted in RPMI to a final concentration of 20 μM. The highest DMSO concentration present in the culture medium was 0.2%. Control cells were treated with DMSO alone at the same concentration present in the test substance being evaluated.

Antibodies (Abs)

Rabbit polyclonal anti-phosphorylated Bcl-2 (Ser-87) and goat polyclonal anti-phosphorylated Bcl-2 (Thr-56) Abs were purchased from Upstate Biotechnology, Inc.; mouse monoclonal anti-Bcl-2, goat polyclonal anti-Bcl-2, rabbit polyclonal anti-p38MAPK, mouse monoclonal anti-poly(ADP-ribose) polymerase (PARP), and rabbit polyclonal anti-Sp1 Abs were purchased from Santa Cruz Biotechnology, Inc. (Santa Cruz, CA). Rabbit monoclonal anti-phosphorylated p38MAPK, rabbit polyclonal anti-phosphorylated MAPKAPK-2 (MAPK-activated protein kinase 2), and rabbit polyclonal anti-MAPKAPK-2 Abs were purchased from Cell Signaling Technology. Mouse monoclonal Abs against the viral NP were purchased from Serotec, and goat polyclonal anti-influenza A virus Abs were purchased from Chemicon. Mouse monoclonal anti-actin and anti-α-tubulin Abs were purchased from Sigma.

Virus Production, Infection, and Titration

Influenza virus A/Puerto Rico/8/34 H1N1 (PR8 virus) and influenza A/NWS/33 H1N1 (NWS virus, ATCC-VR219^{TM}) virus (used in selected experiments only) were grown in the allantoic cavities of 10-day-old embryonated chicken eggs. After 48 h at 37 °C, the allantoic fluid was harvested and centrifuged at 5000 rpm for 30 min to remove cellular debris, and virus titers were determined by a standard plaque assay (26, 27). The titer of the virus preparation was 5×10^7 plaque-forming units/ml.

Cells were challenged 24 h after plating with influenza A virus at a multiplicity of infection (MOI) of 0.05 or, when single-cycle replication was required, 1.5. Mock infection was performed with the same dilution of allantoic fluid from uninfected eggs. Infected and mock-infected cells were incubated for 1 h at 37 °C, washed with PBS, and then incubated with medium supplemented with 2% FBS. The plaque assay was performed according to standard procedures (27, 28) on cell supernatants collected at different times postinfection.

Detection of Apoptosis

Annexin-V Staining—Cells were detached at different time points after infection, stained with Annexin-V-Alexa Fluor, and subjected to fluorescence-activated cell sorting (FACS) with a FACScan flow cytometer (BD Biosciences).

Propidium Iodide Staining—Flow cytometry was performed as previously described (29). Briefly, 24 h postinfection cells were fixed with 70% ethanol at 4 °C for 1 h, washed, and incubated with 250 μg/ml RNase A (Sigma) for 20 min at 37 °C. The cells were then incubated with propidium iodide (PI) (50

μg/ml) for 15 min at 37 °C in the dark. Propidium iodide fluorescence of individual nuclei was measured by FACS, and apoptotic nuclei were identified on a PI histogram of ethanol-treated cells as a hypodiploid peak.

Western Blot Analysis

Cells were washed with cold PBS and centrifuged at 700 × *g* for 10 min. The pellet was lysed in cold lysis buffer (10 mM Tris, 150 mM NaCl, and 0.25% Nonidet P-40, pH 7.4) containing protease and phosphatase inhibitor mixtures. After 30 min on ice, lysates were centrifuged at 10,000 × *g* for 30 min at 4 °C, and their total protein concentrations were determined by the Bradford method (Bio-Rad). Nuclear and cytoplasmic extracts were prepared with the NE-PER^R Nuclear and Cytoplasmic extraction kit (Pierce), and their protein concentrations were determined with the BCA Protein Assay kit (Pierce). Cell lysates or nuclear and cytoplasmic extracts were resuspended in SDS sample buffer containing 10% β-mercaptoethanol, separated with SDS-PAGE, and blotted onto nitrocellulose membranes. The membranes were blocked with 10% nonfat dry milk in PBS for 1 h at room temperature. Primary Abs were used at a final concentration of 1 μg/ml. Secondary Abs were horseradish peroxidase-conjugated (Amersham Biosciences). Blots were developed with an enhanced chemiluminescence system (Amersham Biosciences). For immunoprecipitation studies on the intracellular localization of NP, nuclear and cytoplasmic extracts from equal numbers of PR8-infected MDCK cells were diluted with radioimmune precipitation buffer (50 mM Tris, 150 mM NaCl (pH 7.5), 1% Triton-X, 0.1% SDS, 0.5% sodium deoxycholate. To the same protein concentration, anti-NP Abs (2 μg/ml) were added, and the samples were incubated with protein A-Sepharose (Amersham Biosciences). The immune complexes were washed four times with radioimmune precipitation buffer. The samples were separated by SDS-PAGE, blotted onto nitrocellulose membranes, and stained with anti-influenza virus Abs. Secondary Abs were horseradish peroxidase-conjugated. Blots were developed as described above.

Confocal Laser-scanning Microscopy

For nuclear staining, cell monolayers were washed twice with PBS and fixed with a 4% PBS-buffered paraformaldehyde solution for 30 min at room temperature. After washing, nuclei were stained with 1 μg/ml of DAPI for 15 min at room temperature. Immunofluorescence was assayed in cells that had been fixed with 4% PBS-buffered paraformaldehyde solution for 30 min at room temperature, washed with Tris-buffered saline, and permeabilized for 5 min with 0.1% Triton X-100. After blocking with 1% nonfat dry milk for 30 min, they were incubated with primary and secondary Abs and mounted with the Molecular Probes Antifade kit. The secondary Abs, which were conjugated with Alexa Fluor-488 or tetramethylrhodamine, were purchased from Molecular Probes. Fluorescence was visualized with a confocal laser-scanning microscope (Leica Instruments).

Transfection of Cell Cultures

The full-length human *bcl-2* sequence was amplified by PCR from lysates of freshly isolated human lymphocytes and cloned as a BglII/EcoRI fragment in an enhanced green fluorescent protein (EGFP) pIRES2 vector (pIRES2-EGFP) (Clontech). The following primers were used to obtain the wild-type gene construct: 5′-TTAGATCTATGGCGCACGCTGGGAGAAC-3′ (forward); 5′-CGAATTCTCACTTGTGGCTCAGATAGG-3′ (reverse).

The Δloop plasmid containing the *bcl-2* deletion mutant (Δ40–91 amino acids) was generated with a two-step recombinant PCR with the wild-type construct as a template and two oligonucleotide pairs: 5′-CCACGGGCCCGGCGCCCACAT-CTCCCGC-3′ with 5′-GCAGAGCTGGTTTAGTGAACCG-TCA-3′ and 5′-GGGCCCGTGGTCCACCTGGCCCTCCGC-CAA-3′ with 5′-TATTCCAAGCGGCTTCGGCCAGTAA-3′.

The two PCR products were mixed in the same reaction tube and reamplified with terminal primers. The resulting deleted cDNA was purified, digested with BglII and EcoRI restriction endonucleases, and ligated into the multiple cloning site of pIRES2-EGFP vector. All constructs were verified by sequence analysis.

Lipofectamine (Invitrogen) was used to transfect MDCK cells with pIRES2-EGFP-Bcl-2 and control pIRES2-EGFP vectors. The transfected cells were selected and cloned for ~2 weeks in RPMI supplemented with 10% FBS and 800 μg/ml Geneticin (G418; Invitrogen). The G418-resistant colonies were isolated and subjected to immunofluorescent staining or immunoblotting analysis with anti-human Bcl-2 Abs to detect the expression of EGFP and Bcl-2.

RNA Interference

Down-regulation of Bcl-2 protein expression was induced with small interfering RNA (siRNA), as previously described (30). Briefly, SH-SY5Y cells were transfected with a 21-nucleotide siRNA duplex directed against a target sequence of human Bcl-2 mRNA, 5′-ACACCAGAAUCAAGUGUUCCG-3′ (MWG Biotech, Ebersberg, Germany) or a scrambled siRNA duplex displaying no homology with any other human mRNAs (controls). Transfections were carried out with the Gene Pulser Xcell electroporation system (Bio-Rad), and transfected cells were immediately seeded into fresh medium. The efficiency of siRNA transfections was estimated to be >80% based on the observations of cells cotransfected with siRNAs and nonspecific rhodamine-conjugated oligonucleotides. In time course experiments, Bcl-2 protein expression was found to be maximally down-regulated (−70%) 16 h after siRNA transfection, and full recovery was observed at 24 h. PR8 infection of transfected cells was timed so that the postinfection interval normally characterized by the highest levels of NP in the cytoplasm (6 h postinfection) coincided with peak down-regulation of Bcl-2 expression (16 h post-transfection). The effects of Bcl-2 knockdown on NP localization in infected cells were thus measured at this time point (16 h post-transfection, 6 h postinfection). Its impact on viral production was measured by a plaque assay of cell supernatants 4 h later (20 h post-transfection, 10 h postinfection). This time point was chosen to allow sufficient

time for virions produced during Bcl-2 down-regulation to accumulate in the cell supernatants.

Down-regulation of p38MAPK protein expression was induced with siRNA, as described above. Briefly, MDCK cells were transfected with a 21-nucleotide siRNA duplex directed against a target sequence of canine p38MAPK mRNA, 5′-GGU-CUCUGGAGGAAUUCAAUU-3′ (MWG Biotech, Ebersberg, Germany), or a scrambled siRNA duplex displaying no homology with any other canine mRNAs (controls). Transfections were carried out with the Gene Pulser Xcell Electroporation system (Bio-Rad), and transfected cells were immediately seeded into fresh medium. The efficiency of siRNA transfections was estimated to be >80% based on the observations of cells cotransfected with siRNAs and nonspecific rhodamine-conjugated oligonucleotides. In time course experiments, p38MAPK protein expression was found to be maximally down-regulated (−60%) 20 h after siRNA transfection, and full recovery was observed at 30 h.

Co-immunoprecipitation Studies

PR8-infected or mock-infected MDCKBcl-2 and SH-SY5Y cells (3×10^7) were lysed in 10 mM Hepes, 142.5 mM KCl, 5 mM MgCl$_2$, 1 mM EGTA, and 0.2% Nonidet P-40 (pH 7.5). The total protein concentration was determined by the Bradford method (Bio-Rad), and equal amounts of proteins were immunoprecipitated with 2 μg/ml mouse anti-Bcl-2 or rabbit anti-phosphorylated p38MAPK Abs followed by incubation with protein A-Sepharose (Amersham Biosciences). The immune complexes were washed four times with wash buffer (20 mM Tris, 500 mM NaCl, 0.25% Nonidet P-40, pH 7.2) and once with 20 mM Tris (pH 7.2). The samples were separated by SDS-PAGE, blotted onto nitrocellulose membranes, and stained with anti-p38MAPK or anti-Bcl-2 Abs, as appropriate. Secondary Abs were horseradish peroxidase-conjugated. Blots were developed as described above.

Metabolic Labeling with [^{32}P]Orthophosphate

For *in vivo* metabolic labeling, 10^7 cells were treated for 1 h with SB203580 (20 μM) or DMSO, incubated with PR8 (1.5 MOI) in phosphate-free medium (Eurobio) in the presence of DMSO or SB203580 (1 h at 37 °C), and washed twice with 0.9% NaCl. After an 8-h incubation with 0.5 mCi of [^{32}P]orthophosphate (Amersham Biosciences) in phosphate-free medium supplemented with 2% dialyzed FBS in the presence of DMSO or SB203580, the cells were lysed in 50 mM Tris-HCl (pH 8.0), 150 mM NaCl, and 1% Triton X-100 containing protease and phosphatase inhibitor mixtures. Lysates were immunoprecipitated with 2 μg/ml antiviral NP Abs and separated by 10% SDS-PAGE. Gels were dried and autoradiographed on Eastman Kodak Co. film for 1 week at −80 °C.

Statistical Analyses

Unpaired data were analyzed with Student's *t* test, and *p* values of <0.05 were considered significant. Data are presented as means ± S.D.

The percentage of cytoplasmic NP was calculated as follows: percentage = (number of cells with cytoplasmic NP/(number of cells with cytoplasmic NP + number of cells with nuclear NP)) × 100. Cell counts used for these calculations were based on examination of 10 different fields of each slide.

TABLE 1

Influenza A virus replication and nuclear export of NP in the cell lines used in this study

	Viral titers[a]	Nuclear NP[b]
	pfu/ml	*%*
Bcl-2-negative cells		
MDCK cells	$2.4 \times 10^6 \pm 6 \times 10^5$	21.9 ± 7.1
Bcl-2-expressing cells		
SH-SY5Y cells	$3.2 \times 10^4 \pm 2 \times 10^{4c}$	70.4 ± 8.8^d
MDCK-Bcl-2 cells	$6.9 \times 10^5 \pm 3 \times 10^{5e}$	52.4 ± 4.7^c

[a] Measured in cell supernatant 24 h after PR8 infection and expressed as plaque-forming units per milliliter (pfu/ml).
[b] The percentage of viral NP that was in the nucleus was calculated 24 h after PR8 infection as follows: percentage = (number of cells with nuclear NP/(number of cells with nuclear NP + number of cells with cytoplasmic NP)) × 100. Cell counts used for these calculations were based on examination of 10 different fields of each slide from three different experiments performed in duplicate.
[c] *p* < 0.0001 *versus* MDCK cells.
[d] *p* < 0.00005 *versus* MDCK cells.
[e] *p* < 0.0005 *versus* MDCK cells.

RESULTS

Influenza A Virus Induces the Same Rate of Apoptotic Cell Death in Bcl-2$^+$ and Bcl-2$^-$ Cells—As previously noted, host cell expression of the antiapoptotic protein Bcl-2 has been shown to diminish influenza A virus replication and inhibit the nuclear-cytoplasmic translocation of the viral NP (6, 17). In a preliminary set of experiments, we examined both aspects of the virus life cycle in human neuroblastoma cells (SH-SY5Y), which constitutively express high levels of Bcl-2, and MDCK cells, where constitutive Bcl-2 expression is undetectable (6). The latter cells were evaluated after stable transfection with a vector encoding the wild-type Bcl-2 protein (MDCKBcl-2 cells) or with an empty vector (referred to hereafter simply as MDCK cells). As shown in Table 1, much higher percentages of viral NP remained in the nucleus in PR8-infected Bcl-2$^+$ cells, and, as a consequence, viral replication in these cells was significantly inferior to that observed in Bcl-2$^-$ cells.

To determine whether these effects are related to the antiapoptotic function of Bcl-2, we compared PR8-induced apoptosis in the same three cell lines. FACS analysis of Annexin-V staining showed that the kinetics of influenza A virus-induced apoptosis were similar in Bcl-2$^+$ and Bcl-2$^-$ cells (Fig. 1*A*); 8, 18, and 24 h postinfection, there were no significant differences between the percentages of apoptotic cells in the three cell lines. Analysis of nuclear DAPI staining 24 h postinfection confirmed that the rates of apoptosis in Bcl-2$^+$ and Bcl-2$^-$ cells were similar (Fig. 1*B*). Immunoblots of nuclear extracts from infected cells of all three lines revealed cleavage of PARP (Fig. 1*C*), a marker of the caspase-3-like enzyme activation that underlies active apoptosis. These experiments demonstrate that influenza A virus-induced apoptosis is not prevented by the Bcl-2 protein. Our next objective was to identify the mechanism(s) underlying this phenomenon.

Influenza A Virus-induced Apoptosis in Bcl-2$^+$ Cells Is Related to Bcl-2 Phosphorylation by p38MAPK—Several studies have demonstrated that the antiapoptotic potential of Bcl-2 is diminished by phosphorylation of serine and threonine residues in the loop between the protein's BH4 and BH3 domains
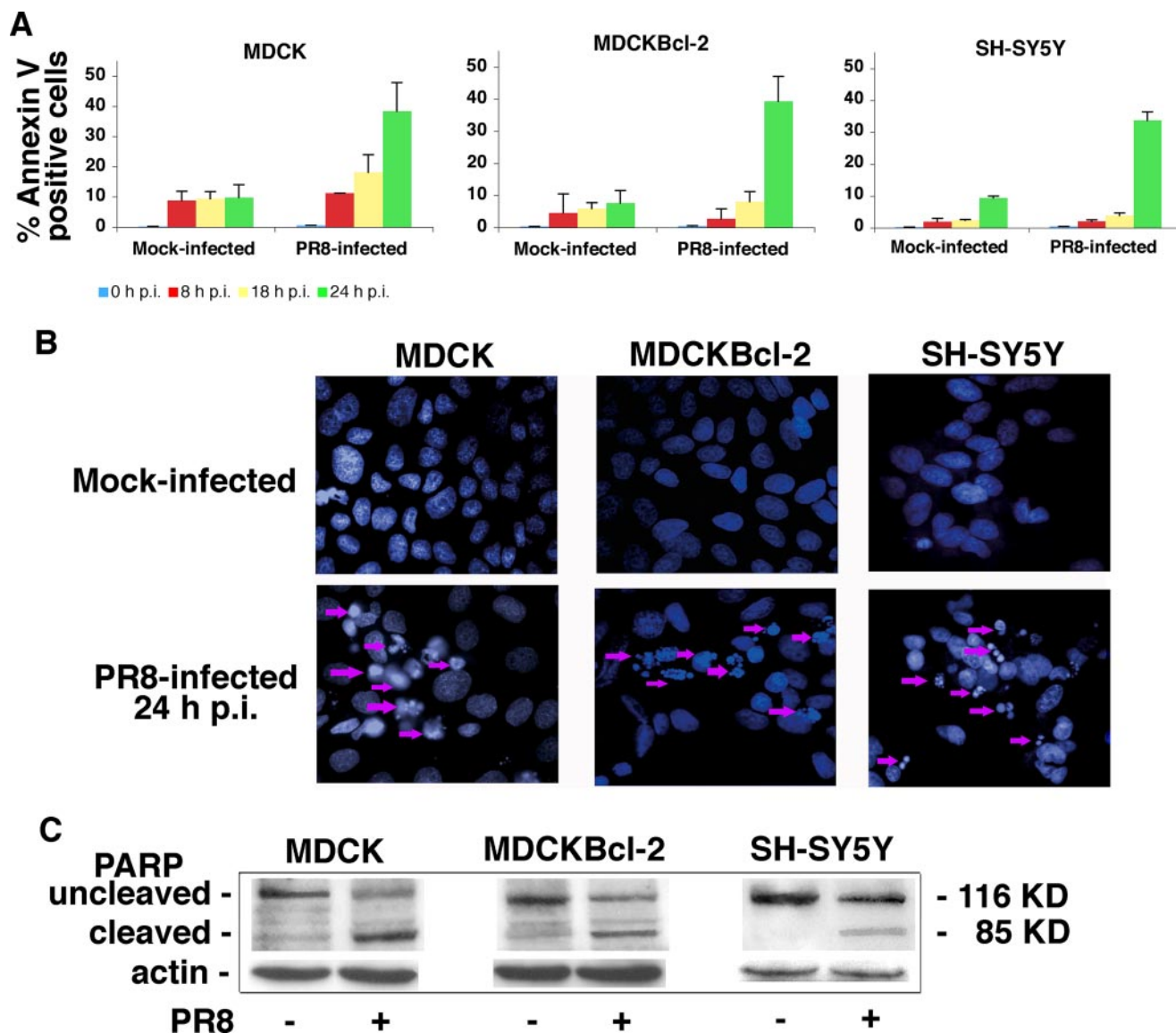
FIGURE 1. **Influenza A virus infection induces similar rates of apoptosis in Bcl-2$^+$ and Bcl-2$^-$ cells.** *A*, MDCK, MDCKBcl-2, and SH-SY5Y cells were collected 8, 18, and 24 h postinfection (*p.i.*) (mock or with PR8), stained with Annexin-V-Alexa Fluor, and subjected to FACS to quantitatively assess apoptosis. The percentages shown represent the mean $\pm$ S.D. ($n = 6$) result of three individual experiments, each performed in duplicate. *B*, fluorescence microscopy of PR8-infected and mock-infected MDCK, MDCKBcl-2, and SH-SY5Y cells fixed and stained with DAPI dye 24 h after PR8 or mock infection. The *arrows* indicate apoptotic cells. Annexin-V and DAPI staining patterns were similar when cells were infected with influenza virus A/NWS/33 (data not shown). *C*, caspase-3-like activity reflected by PARP cleavage in the nuclei of PR8- and mock-infected MDCK, MDCKBcl-2, and SH-SY5Y cells. Nuclei were isolated from cells collected 24 h postinfection. Nuclear extracts (total protein content, 50 μg) were subjected to SDS-PAGE, blotted, and immunostained with anti-PARP Abs. Loading control was actin. Results are shown for one representative experiment of three performed.

(12–15, 31), and influenza A virus is known to activate several serine-threonine kinase pathways in the host cell, including the p38MAPK (32, 33) and Raf/MEK/ERK cascades (5). We speculated, therefore, that viral activation of the p38MAPK or ERK pathway in Bcl-2$^+$ cells might result in phosphorylation of Bcl-2, which would reduce the protein's ability to protect the host cell from virus-induced apoptosis. To test this hypothesis, we infected MDCKBcl-2 cells with PR8 in the presence of SB203580, a pyridyl-imidazole inhibitor of p38MAPK (34), or U0126, which specifically inhibits MEK (35). Twenty-four hours postinfection, cells were subjected to mobility shift analysis/Western blot analysis to assess Bcl-2 phosphorylation. As shown in Fig. 2*A*, PR8 infection was associated with a clear shift to the 29-kDa form of Bcl-2, which is indicative of phosphoryl-

ation (14–16), and this effect was clearly attenuated (−71%) by SB203580 but unaffected by U0126 (Fig. 2*B*). Our next step was to assess the phosphorylation status of the Thr-56 and Ser-87 residues in Bcl-2 following influenza A virus infection. These residues are known targets of p38MAPK, and their phosphorylation is associated with a decrease in the antiapoptotic capacity of Bcl-2 (15). As shown in Fig. 2*C*, lysates from PR8-infected MDCKBcl-2 cells reacted positively with antibodies directed specifically against phosphorylated forms of Thr-56 and Ser-87, and phosphorylation of these residues was markedly attenuated by the presence of SB203580 (mean reductions compared with DMSO-treated controls: 63% $\pm$ 13% at Thr-56, 71% $\pm$ 15% at Ser-87). These results demonstrated that PR8 infection of Bcl-2$^+$ cells causes phosphorylation of the antiapoptotic pro-
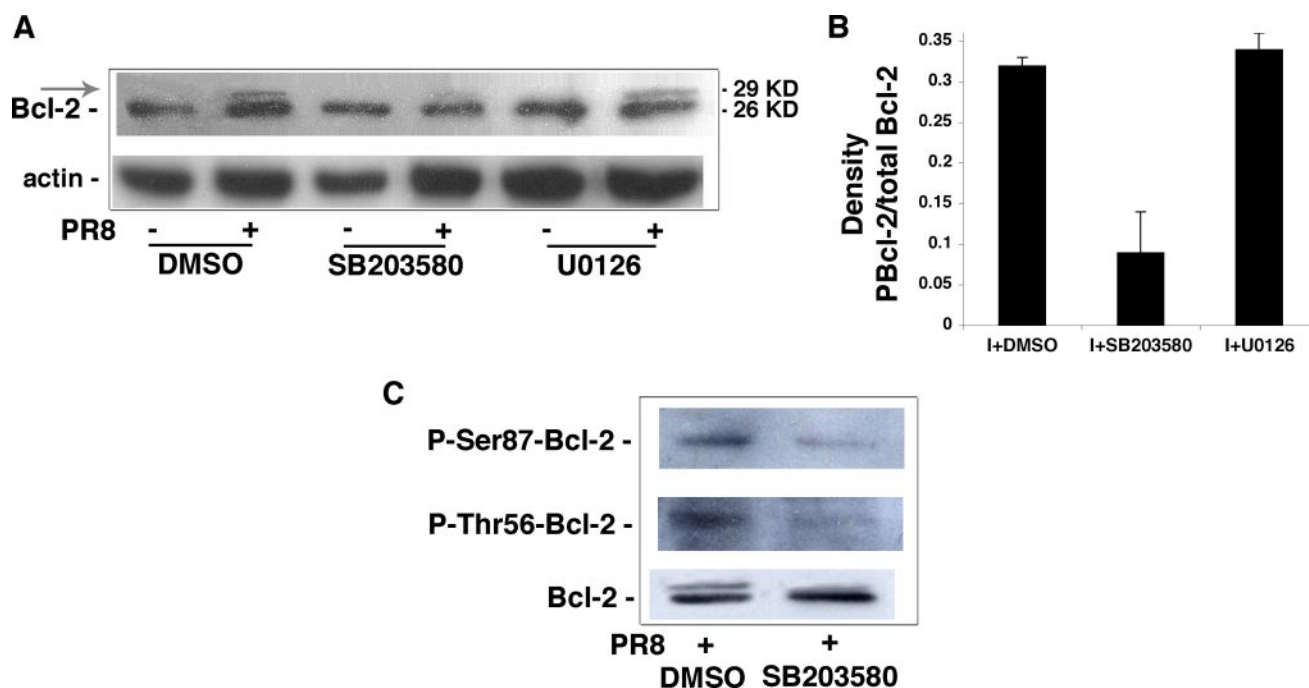
FIGURE 2. **Influenza A virus infection results in phosphorylation of Bcl-2 by p38MAPK.** *A*, MDCKBcl-2 cells were treated continuously with 20 μM SB203580, 20 μM U0126, or DMSO (controls) 1 h before and 24 h after PR8 or mock infection. Lysates treated with phosphatase-inhibitor mixtures were subjected to 15% SDS-PAGE with a large vertical electrophoresis system, blotted, and immunostained with anti-Bcl-2 Abs. The membrane was then stripped and restained with anti-actin Abs as a loading control. The shift from the native 26-kDa Bcl-2 protein to the 29-kDa form (*arrow*) is indicative of phosphorylation. Western blots are shown for one representative experiment of three performed. There was no evidence of cross-reactivity between the anti-influenza Abs and the shifted band or between anti-Bcl-2 Abs and the viral proteins from our influenza A PR8 preparations (data not shown). *B*, densitometric analysis of three different experiments shown in *A*. Results are expressed as ratios of phosphorylated Bcl-2 to total Bcl-2. *C*, PR8-infected MDCKBcl-2 cells were treated continuously with 20 μM SB203580 or DMSO (controls) 1 h before and 24 h after PR8 infection (*I*). Lysates were subjected to SDS-PAGE and immunoblotted with antibodies to Bcl-2 (loading controls) or to phosphorylated forms of the protein's Thr-56 and Ser-87 residues. Results are shown for one representative experiment of four performed.

tein, which can be attributed to the action of virus-activated p38MAPK at Thr-56 and Ser-87.

Several lines of *in vitro* evidence (13–15) indicate that p38MAPK-mediated phosphorylation of Bcl-2 is also involved in the apoptosis provoked in various cell types by the withdrawal of survival factors. We reasoned that the same phosphorylation event might also be causally linked to the apoptosis triggered by influenza A virus infection in Bcl-2$^+$ cells. To test this hypothesis, we first assessed virus-induced apoptosis in MDCKBcl-2 and MDCKBcl-2Δloop cells (*i.e.* MDCK cells that had been stably transfected with a Bcl-2 deletion mutant, which encodes a 19-kDa protein lacking the loop region where the MAPK-phosphorylatable residues are found). As shown in Fig. 3*A*, the two cell lines expressed similar amounts of their respective Bcl-2 proteins. FACS assessment of PI fluorescence and immunoblot analysis of PARP cleavage both revealed significantly lower rates of apoptosis in the MDCKBcl-2Δloop cells (Fig. 3, *B* and *C*), suggesting that the ability of the influenza A virus to induce apoptosis in Bcl-2-expressing cells is at least partly dependent on the presence of Bcl-2 residues that can be phosphorylated by MAPK. The close link between Bcl-2 phosphorylation, particularly that mediated by p38MAPK, and influenza A virus-induced apoptosis in Bcl-2$^+$ cells also emerged from experiments with MDCKBcl-2 cells infected in the presence of different concentrations of SB203580. As shown in Fig. 3*D*, FACS analysis of these cells revealed that this specific p38MAPK inhibitor significantly diminished virus-induced apoptosis (compared with DMSO-treated control cells),

especially when used at a concentration of 20 μM. In contrast, SB202474 (an inactive SB203580 analog) or PD98059 (which specifically inhibits the MEK/ERK pathway) did not significantly inhibit PR8-induced apoptosis. Collectively, these findings suggest that p38MAPK-mediated phosphorylation of Bcl-2 is likely to be an important factor in the ability of the influenza virus to overcome the antiapoptotic properties of Bcl-2$^+$ cells.

Influenza Virus-activated p38MAPK Is Distributed Differently in Bcl-2$^+$ and Bcl-2$^-$ Cells—The active form of p38MAPK is found mainly in the nucleus, but smaller amounts are also present in the cytosol, where the kinase has several potential substrates, including Bcl-2 (13, 25). Therefore, to provide additional evidence of p38MAPK/Bcl-2 interaction during influenza virus infection, we compared the intracellular distributions of the kinase in MDCK, MDCKBcl-2, and SH-SY5Y cells infected with a high MOI (1.5) of PR8 (to allow single-cycle replication). In both Bcl-2$^+$ cell lines, confocal microscopy revealed large amounts of active p38MAPK in the cytoplasm, where it clearly colocalized with Bcl-2, whereas the activated p38MAPK in MDCK cells was found predominantly in the nucleus (Fig. 4*A* and supplemental Fig. 1). Moreover, direct interaction between the two proteins during infection was documented in coimmunoprecipitation assays (Fig. 4*B*), suggesting that binding between p38MAPK and Bcl-2 might prevent the enzyme from migrating to the nucleus. We also found that MAPKAPK-2, the nuclear target of p38MAPK, was phosphorylated in PR8-infected MDCK cells, and its phosphorylation
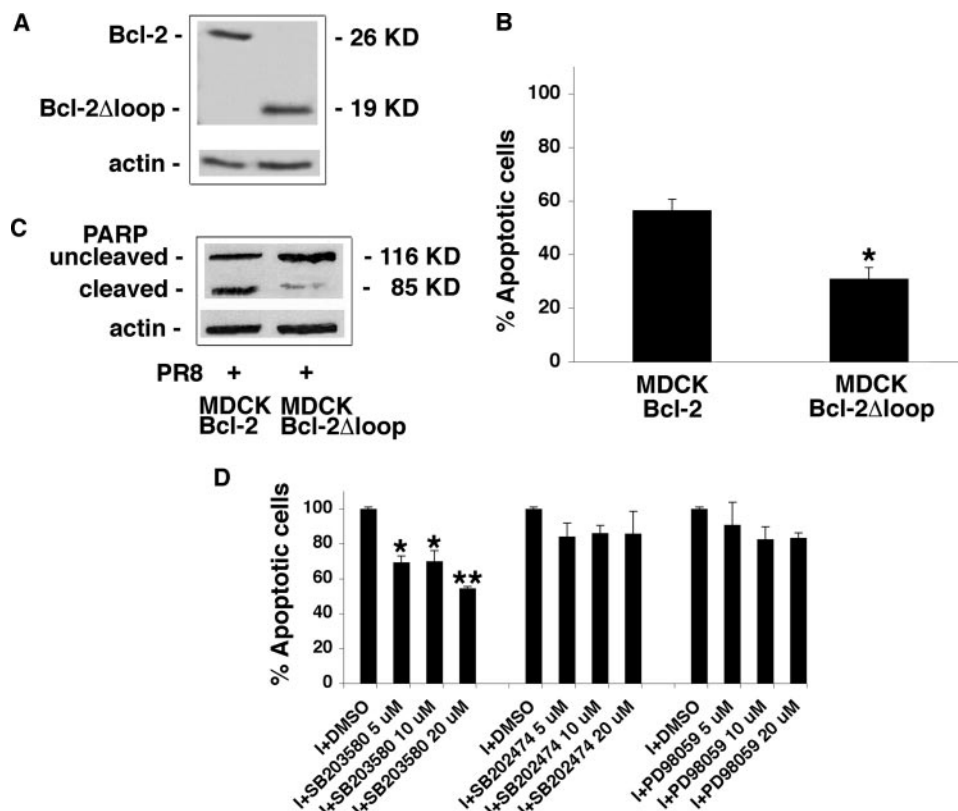
FIGURE 3. **The ability of influenza A virus to induce apoptosis in Bcl-2$^+$ cells is related to Bcl-2 phosphorylation by p38MAPK.** *A*, total protein extracts (50 μg) from MDCKBcl-2 and MDCKBcl-2Δloop cells were subjected to SDS-PAGE, blotted, and stained with goat anti-Bcl-2 Abs capable of recognizing both the wild type and loop-deleted Bcl-2 proteins. Actin was used as a loading control. The effect of Bcl-2 loop deletion on virus-induced apoptosis was then evaluated with three techniques in MDCKBcl-2 and MDCKBcl-2Δloop cells 24 h after PR8 infection: *B*, PI nuclear fluorescence was measured by FACS in infected MDCKBcl-2 and MDCKBcl-2Δloop cells. Each value shown represents the mean $\pm$ S.D. ($n = 10$) of results from five separate experiments, each performed in duplicate. *, $p < 0.05$ *versus* MDCKBcl-2 cells. *C*, PARP cleavage was assessed in nuclear extracts (equal amounts) from both cell lines. Extracts were subjected to SDS-PAGE, blotted, and immunostained with anti-PARP Abs. Actin was used as loading control. *D*, PI nuclear fluorescence was measured by FACS in infected MDCKBcl-2 cells treated continuously with different concentrations (5-10-20 μM) of SB203580, SB202474, PD98059, or DMSO (controls) 1 h before and 24 h after infection (*I*). The percentage of apoptotic cells among those treated with DMSO was considered as 100%. Each value shown represents the mean $\pm$ S.D. ($n = 4$) of results from two separate experiments, each performed in duplicate. *, $p < 0.05$; **, $p < 0.005$ *versus* I + DMSO.

was inhibited by SB203580-treatment. In contrast, MAP-KAPK-2 phosphorylation was strongly reduced in infected MDCKBcl-2 cells (Fig. 4*C*). The substrates being phosphorylated by p38MAPK in Bcl-2$^+$ and Bcl-2$^-$ cell populations infected with the influenza virus may thus be located in different subcellular compartments. In line with these findings, when constitutive Bcl-2 expression in SH-SY5Y cells was down-regulated with siRNA (for more details, see "RNA Interference"), active p38MAPK was found predominantly in the nucleus of infected cells (Fig. 4*D*). The high cytoplasmic levels of the kinase and its demonstrated interaction with Bcl-2 in the infected cells that expressed this protein are fully consistent with our contention that the antiapoptotic protein is phosphorylated by virally activated p38MAPK. Equally intriguing, however, is the relative absence of p38MAPK activity in the nucleus of these cells, where it is known to perform a multitude of important functions.

Interaction between Bcl-2 and p38MAPK May Also Affect Nuclear Export of the vRNP and Viral Replication—Previous studies have demonstrated that nuclear-cytoplasmic transloca-

tion of the vRNP (6) and viral replication (6, 17) are impaired in Bcl-2$^+$ cells. We confirmed these alterations (Table 1) and demonstrated that they are indeed related to the host cell's expression of Bcl-2. In experiments based on the siRNA technique described in the legend to Fig. 5, down-regulation of Bcl-2 expression in SH-SY5Y cells markedly increased the percentage of NP present in the cytoplasm, as shown by an immunofluorescence assay (66.3 $\pm$ 3.5% *versus* 21.6 $\pm$ 7.2% in si Scr cells); Western blot analysis (densitometric analysis of NP expression, si Bcl-2/si Scr ratios = 2.5/1 for cytosolic NP, 0.5/1 for nuclear NP); and the viral titers found in cell supernatants (for details on the timing of these assays, see "RNA Interference").

These findings, along with the diminished presence and activity of p38MAPK observed in the nuclei of Bcl-2$^+$ cells (Fig. 4, *C* and *D*), raised the possibility that p38MAPK might also affect the nuclear export of vRNPs, which is known to depend on NP phosphorylation (5, 18, 19). To evaluate this hypothesis, we performed immunofluorescence assays to investigate the intracellular location of NP in PR8-infected MDCK cells (Fig. 6*A*). In these Bcl-2$^-$ cells, NP was located in the cytoplasm 8 h postinfection, but when the cells were infected during SB203580-in-

duced inhibition of p38MAPK, NP remained largely confined to the nuclei through postinfection hour 8. This nuclear retention was not seen when SB203580 was replaced with its inactive analog SB202474. The same picture emerged when the NP was immunoprecipitated from the cytoplasmic and nuclear compartments of infected cells. As shown in Fig. 6*A*, densitometric analysis of immunoprecipitated NP revealed that the protein nuclear levels were higher in infected cells treated with 10 or 20 μM SB203580 than in untreated cells and in those treated with SB202474. In line with these findings, siRNA knockdown of p38MAPK expression in MDCK cells prevented NP translocation to the cytosol, as shown by immunofluorescence assay and Western blot analysis (Fig. 6*B*).

Next, to determine whether p38MAPK is involved in the phosphorylation of NP, we performed immunoprecipitation experiments on [^{32}P]orthophosphate-labeled cells. The amount of phosphorylated NP precipitated from MDCKBcl-2 cells was markedly lower than that obtained from MDCK cells (Fig. 7*A*), which indicates that phosphorylation of this viral protein is diminished in Bcl-2$^+$ cells. A similar decrease in NP
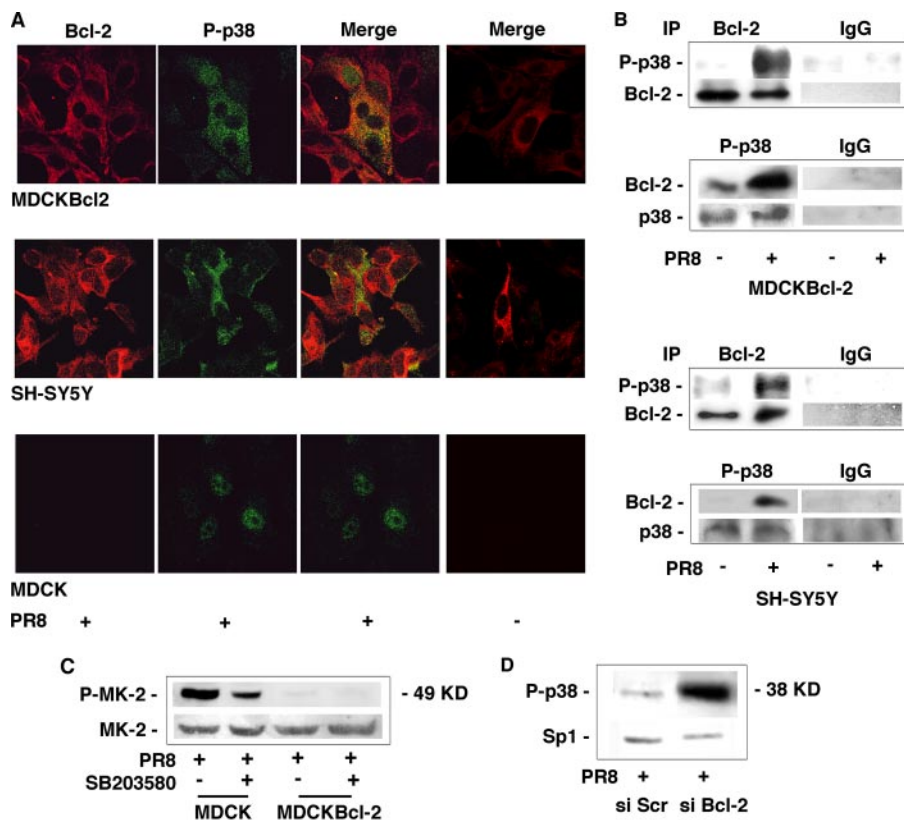
FIGURE 4. **Activated p38MAPK is found predominantly in the cytoplasm of influenza A virus-infected Bcl-2-expressing cells, where it binds with Bcl-2.** *A*, confocal microscopic images of MDCKBcl-2, SH-SY5Y, and MDCK cells collected 8 h after infection with PR8 (MOI 1.5), fixed, and labeled with antibodies against Bcl-2 (*Bcl-2*) or phosphorylated p38MAPK (*P-p38*) (*first* and *second columns* from the *left*, respectively). *Merged images* for each infected cell line are shown in the *third column*. Results are shown for one representative experiment of three performed. *Merged images* for mock-infected control cells are presented in the *fourth column*. *B*, lysates from PR8-infected or mock-infected MDCKBcl-2 and SH-SY5Y cells were immunoprecipitated (*IP*) with anti-Bcl-2 (*Bcl-2*) or anti-phospho-p38MAPK (*P-p38*) Abs, run on SDS-PAGE, blotted, and immunostained with anti-phospho-p38MAPK or anti-Bcl-2 Abs, respectively. As a control of immunoprecipitation, the same nitrocellulose filters were stripped and restained with anti-Bcl-2 or anti-p38MAPK Abs. MDCKBcl-2 and SH-SY5Y lysates from PR8-infected or mock-infected cells were immunoprecipitated with mouse IgG or rabbit IgG, as control. *C*, nuclear extracts from MDCK and MDCKBcl-2 cells treated continuously with 20 μM SB203580 or DMSO (controls) for 1 h before and 24 h after PR8 infection were subjected to SDS-PAGE and immunoblotted with antibodies against phosphorylated MAPKAPK-2 (*P-MK-2*). The same nitrocellulose filter was then stripped and restained with anti-MAPKAPK-2 (*MK-2*) Abs. *D*, nuclear extracts from infected SH-SY5Y cells, transfected with siRNA against Bcl-2 (*si Bcl-2*) or with scrambled siRNA (*si Scr*), were subjected to SDS-PAGE and immunoblotted with antibodies against phosphorylated p38MAPK (*P-p38*). The same nitrocellulose filter was then stripped and restained with anti-Sp1 Abs. Results are shown for one representative experiment of two performed.

Our final set of experiments focused on the implications of the above findings in terms of influenza virus replication. As shown in Fig. 7D (*top*), the viral yields of supernatants from PR8-infected MDCK cells dropped by ~1 log after treatment with 20 μM SB203580, whereas it was unaffected by SB202474 treatment. The dose of 10 μM p38MAPK inhibitor caused a less pronounced reduction of viral replication. Such a result seems to be not completely in line with the picture emerging from Fig. 6A, in which the same dose of SB203580 caused an evident impairment of NP nuclear export. Further studies are in progress to clarify this apparent discrepancy. As already reported for 1 and 2.5 μM (36, 37), the dose of 5 μM SB203580 did not affect viral replication (data not shown). Similar results were observed in MDCK cells infected with NWS virus (data not shown). Even at the highest concentration used, SB203580 had no effect on cell morphology or viability, which tends to exclude cytotoxicity as a mechanism underlying its reduction of viral replication (data not shown). Indeed, this reduction appears to be directly related to inhibition of p38MAPK activity, since decreased viral yields were also observed after siRNA-induced down-regulation of the expression of this kinase (Fig. 7D, *bottom*). Collectively, the findings reported above strongly suggest that interaction between Bcl-2 and p38MAPK during influenza virus infection has important implications not only for host cell apoptosis but also for the nuclear export of the vRNPs and for viral replication.

phosphorylation occurred in MDCK cells treated with SB203580 (Fig. 7A). (As shown in Fig. 7B, the p38MAPK inhibitor itself had no significant effect on the expression of NP or other viral proteins.) Additional experiments (Fig. 7C) showed that in MDCK cells, activated p38MAPK and viral NP colocalize in the nucleus during the early phase of infection. Later, the NP moves into the cytoplasm, whereas p38MAPK remains in the nucleus (through the 8th hour postinfection). In contrast, in MDCKBcl-2 cells, activated p38MAPK was found mainly in the cytoplasm at all time points, and 8 h after infection, the NP was still confined to the nucleus. These findings suggest that in Bcl-2$^-$ cells, influenza virus-activated p38MAPK freely translocates into the nucleus, where it contributes to the processes of NP phosphorylation and nuclear vRNP export. These events do not seem to occur in Bcl-2$^+$ cells, where the active form of the kinase is confined for the most part to the cytoplasm as a result of its interaction with Bcl-2.

DISCUSSION

In this paper, we demonstrate that host cell expression of Bcl-2 and its interaction with p38MAPK negatively affect replication of the influenza A virus while facilitating virally induced apoptosis. The presence of Bcl-2 is generally recognized to protect cells against apoptotic death induced by different stimuli, including viral infection (12, 38). The role of apoptotic cell death in the pathogenesis of viral infection is a matter of great debate. Interestingly, some viruses inhibit host cell apoptosis with several mechanisms, including the expression of Bcl-2 homologs. By preventing the premature death of its host, the virus allows itself to replicate and to establish persistent infec-
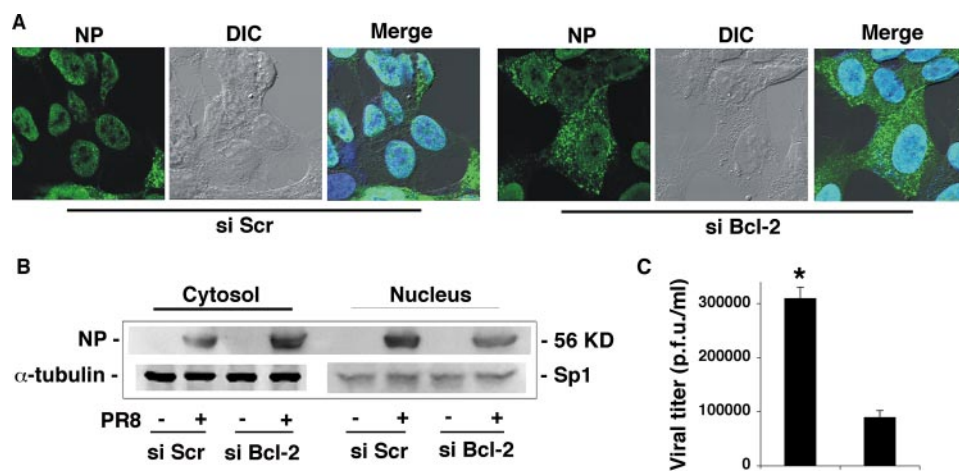
FIGURE 5. **Bcl-2 knockdown in host cells increases influenza A viral replication and vRNP export.** SH-SY5Y cells were transfected with siRNA against Bcl-2 (*si Bcl-2*) or with scrambled siRNA (*si Scr*), and 9 h later, the transfected cells were infected with a high MOI (1.5) of PR8 (to allow single-cycle viral replication). *A*, 6 h postinfection (16 h post-transfection, when down-regulation of Bcl-2 expression in si Bcl-2 cells peaked), the cells were fixed, labeled with anti-NP Abs, and analyzed by confocal microscopy. Phase-contrast and differential interference contrast (*DIC*) microscopy images and images of DAPI-stained nuclei were used as controls. *Merged images* are presented for both cell lines. *B*, cytosolic and nuclear extracts from si Bcl-2 and si Scr cells were subjected to SDS-PAGE and immunoblotted with antibodies against influenza virus. The same nitrocellulose filter was then stripped and restained with anti-α-tubulin or with anti-Sp1 Abs. Results are shown for one representative experiment of two performed. *C*, supernatant samples from infected si Bcl-2 and si Scr cells were collected 10 h after infection (20 h post-transfection) and analyzed for infectious virions by plaque assay. Data represent the mean $\pm$ S.D. ($n = 4$) of results from two separate experiments, each performed in duplicate. *, $p < 0.05$ *versus* si Scr cells. *p.f.u.*, plaque-forming units.

tions. On the contrary, other viruses induce apoptosis of infected cells by several mechanisms, including Bcl-2 destabilization, and this event can be involved in viral dissemination (39).

Here we demonstrate that influenza A virus infection produces similar rates of apoptosis in Bcl-2$^-$ and Bcl-2$^+$ cells, and our findings indicate that this phenomenon is related to viral activation of p38MAPK, which causes phosphorylation of the antiapoptotic protein (Figs. 1 and 2). In several contexts, phosphorylation of Bcl-2 profoundly alters its ability to counteract apoptosis triggered by various stimuli (13–15, 31). Whether the antiapoptotic potential is enhanced or diminished depends on the kinase responsible for the phosphorylation, the sites it targets, and the conformational changes that are produced. Phosphorylation of the Bcl-2 Thr-56 and Ser-87 residues, which are the specific targets of p38MAPK, is consistently followed by apoptotic death in cells subjected to serum withdrawal (15), and these same residues are phosphorylated by p38MAPK following influenza virus infection (Fig. 2*C*). The importance of this event in the virus ability to induce programmed cell death in Bcl-2$^+$ cells is supported by the markedly reduced rates of virally triggered apoptosis observed in cells that expressed an unphosphorylatable mutant form of Bcl-2 (Fig. 3, *B* and *C*) and by the similar reductions occurring when the infected cells were treated with a specific inhibitor of p38MAPK (Fig. 3*D*). These findings delineate a new apoptotic pathway that is activated by influenza virus in Bcl-2$^+$ cells.

Although expression of Bcl-2 does not protect host cells from influenza virus-induced apoptosis, it correlates with a reduced viral replication and with impaired export of vRNPs from the nucleus to the cytoplasm (6). This essential step in the life cycle of the virus is reportedly mediated by the cell export machinery,

which involves CRM-1 (chromosome region maintenance protein 1), and by the M1 (viral matrix) and NEP (nuclear export) proteins (40–43). It is well documented that phosphorylation of vRNPs influences their nuclear transport (44), possibly by altering their binding affinity for M1 (reviewed in Ref. 3). Viral RNP traffic is also reportedly modulated by several cellular proteins and kinase signaling pathways, including the protein kinase C and MAPK cascades (4–9, 45). Pleschka *et al.* (5), for example, reported that the ERK inhibitor U0126 inhibits both vRNP traffic and virus production, although it does not appear to have a direct effect on NP phosphorylation.

Our study provides multifaceted evidence of the involvement of the p38MAPK pathway in the regulation of vRNP translocation from the nucleus to the cytosol. First of all, prior to its export to the cytoplasm, NP colocalizes with p38MAPK in the nucleus of infected cells that do not express Bcl-2 (Fig. 7*C*). Second, selective suppression of p38MAPK activity with SB203580 impairs phosphorylation of NP (Fig. 7*A*), nucleocytoplasmic translocation of vRNPs (Fig. 6), and overall viral replication (Fig. 7*D*), without affecting viral protein synthesis (Fig. 7*B*). Similar effects are produced by siRNA-mediated down-regulation of p38MAPK expression (Figs. 6*B* and 7*D*, *bottom*). Although inhibition of p38MAPK activity alone was not sufficient to block all viral replication, the reduction achieved with 20 μM SB203580 or p38MAPK knockdown amounted to ~1 log, similar to those described by other groups after treatment with specific inhibitors of MEK (5) or phosphatidylinositol 3-kinase/Akt (9) signaling pathways. It would thus appear that the control of vRNP traffic depends on more than one phosphorylative event. In fact, stronger inhibition of influenza virus replication and nuclear retention of vRNPs have been obtained with less specific protein kinase inhibitors (4), such as the broad spectrum inhibitor H7 (46) or the natural polyphenol resveratrol (47), which suppresses protein kinase C activity and that of the protein kinase C-dependent c-Jun N-terminal kinase and p38MAPK pathways and also inhibits viral protein synthesis (7). The fact that H7 and resveratrol both inhibit p38MAPK supports our contention that this kinase promotes viral replication; the fact that both also have other effects would account for their more marked suppression of viral replication. In this scenario, it is reasonable to imagine p38MAPK modulating NP phosphorylation status, thereby altering the affinity of the vRNP for M1 binding and hindering its nuclear export by CRM-1. However, other cellular factors probably affect influenza virus replication through mechanisms that are independent of the chain of events just hypothesized. Wurzer *et al.* (8)
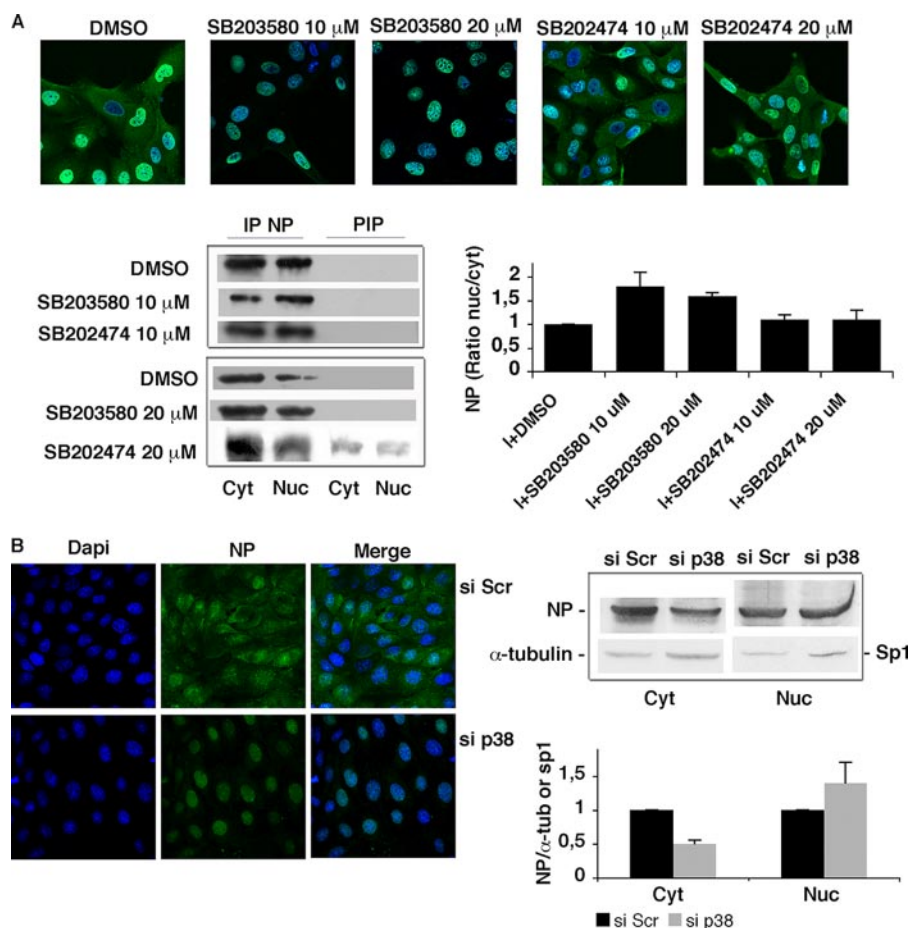
FIGURE 6. **p38MAPK plays a role in the nucleocytoplasmic export of NP.** *A*, *top*, MDCK cells were treated continuously with different concentrations (10–20 μM) of SB203580, SB202474, or DMSO (controls) 1 h before PR8 infection (*I*) (1.5 MOI). At postinfection hour 8, cells were collected, fixed, labeled with anti-NP Abs (*green fluorescence*), subjected to nuclear DAPI staining (*blue staining*), and analyzed by confocal microscopy. *Merged images* of the infected cells are shown in the figure. Results are shown for one representative experiments of two performed. *Bottom*, equal numbers of MDCK cells were treated as described before. At postinfection hour 8, cytosolic and nuclear extracts were immunoprecipitated (*IP*) with anti-NP Abs, subjected to SDS-PAGE and immunoblotted with anti-influenza virus Abs. *PIP*, postimmunoprecipitation supernatants. Densitometric analysis of NP expression is shown on the *right*. Results are expressed as mean ratio of nuclear NP to cytosolic NP $\pm$ S.D. from two separate experiments. *B*, *left*, MDCK cells were transfected with siRNA against p38MAPK (*si p38*) or with scrambled siRNA (*si Scr*), and 12 h later the transfected cells were infected with PR8 (1.5 MOI). Eight hours postinfection (21 h post-transfection, when down-regulation of p38MAPK expression in si p38 cells peaked), cells were collected, fixed, labeled with anti-NP Abs (*NP*), subjected to nuclear DAPI staining (*Dapi*), and analyzed by confocal microscopy. *Merged images* are shown for each condition in the *third column*. Results are shown for one representative experiment of two performed. *Right*, si p38 and si Scr cells were infected with PR8, and 8 h after infection (21 h post-transfection), cytosolic and nuclear extracts were subjected to SDS-PAGE and immunoblotted with anti-influenza A virus Abs. *Bottom*, densitometric analysis of NP expression. Results are expressed as mean ratio of cytosolic NP to α-tubulin $\pm$ S.D. and nuclear NP to Sp1 $\pm$ S.D. from two separate experiments.

of Bcl-2$^+$ or Bcl-2$^-$ cells; in the latter case, p38MAPK is entirely addressed to the nucleus, whereby it efficiently participates in vRNP phosphorylation. In fact, the impaired viral replication and vRNP nucleocytoplasmic translocation observed in Bcl-2$^-$ cells treated with SB203580 are identical to those seen in untreated Bcl-2$^+$ cells (6). Together with the enhanced vRNP nuclear export and viral replication we observed in Bcl-2-silenced SH-SY5Y cells (Fig. 5), these findings suggest that Bcl-2 is a preferential substrate of activated p38MAPK, and when it is expressed in the cytoplasm of a cell infected by influenza virus, a substantial proportion of the kinase localizes in the cytoplasm and combines with the antiapoptotic protein (Fig. 4*B*). The resulting decrease in nuclear kinase activity (Fig. 4*C*) could explain the impaired NP phosphorylation and viral replication observed in Bcl-2-positive cells. This chain of events is compatible with our original hypothesis that Bcl-2 inhibition of influenza viral replication is related to its interference with the p38MAPK phosphorylation pathway. A similar phenomenon has been described for Herpes simplex virus type-1. This virus also activates p38MAPK during infection, but it uses specific viral proteins to prevent the kinase from destabilizing Bcl-2 and provoking the apoptotic death of the host (48). In other words, Herpes simplex virus type-1 has developed strategies for promoting its own replication by activating p38MAPK and for overcoming host cell responses mediated by Bcl-2. In this scenario, our findings suggest that Bcl-2 may represent a component of the antiviral response of some cells, a "weapon" that sabotages viral replication by interacting with one or more of the cellular factors needed for this process, namely p38MAPK. This line of defense may be overcome by genetically sophisticated viruses like Herpes simplex virus type-1, but for other viruses (the influenza virus in particular), it might effectively render Bcl-2-expressing cells less permissive to the infection.

reported, for example, that inhibition of caspase-3 activity diminishes vRNP export as well as viral replication. However, this mechanism does not appear to be responsible for the differences in viral replication that we observed between Bcl-2$^+$ and Bcl-2$^-$ cells, since PARP cleavage, a marker of caspase-3-like activation, was observed after viral infection of all of the cell lines we examined.

The existence of a cytosolic/mitochondrial substrate in addition to multiple nuclear targets of p38MAPK delineates a dual scope embedded in its physiology; the final amount of active enzyme directed to the nucleus is largely determined by whether its cytosolic target is significantly expressed or not. This duality becomes particularly evident upon viral infection

It is possible, of course, that other mechanisms are also responsible for the reduced viral replication occurring in Bcl-2$^+$ cells. Olsen *et al.* (17) have shown, for example, that the decreased virus production in these cells is associated
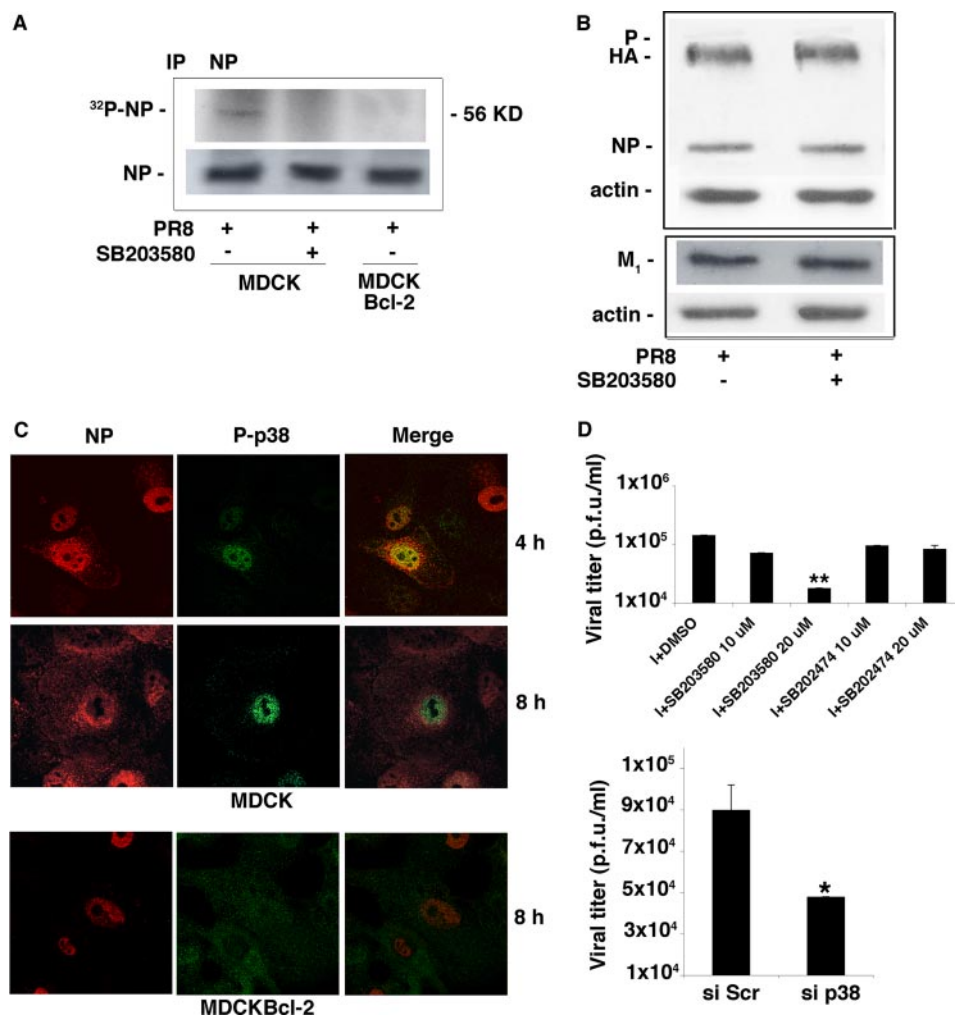
FIGURE 7. **p38MAPK contributes to the phosphorylation of NP.** *A*, PR8-infected (1.5 MOI) MDCK cells treated continuously with 20 μM SB203580 or DMSO and untreated infected MDCKBcl-2 cells were metabolically labeled with $^{32}PO_4$. Eight hours postinfection, cell lysates were immunoprecipitated (*IP*) with anti-NP Abs. The precipitates were subjected to SDS-PAGE and autoradiographed (*upper gel*). Equal amounts of the cell lysates immunoprecipitated with anti-NP Abs and subjected to SDS-PAGE were immunoblotted with anti-influenza A virus Abs (*lower gel*). *B*, lysates from DMSO- and SB203580-treated, PR8-infected (1.5 MOI) MDCK cells were subjected to SDS-PAGE, blotted, and stained with anti-influenza A virus Abs. The same nitrocellulose filters were then stripped and restained with anti-actin Abs. C, *top* and *middle*, MDCK cells were infected with PR8 (1.5 MOI). Four and eight hours later, the cells were fixed, labeled with anti-NP Abs (*NP*) and anti-phospho-p38MAPK Abs (*P-p38*), and analyzed by confocal microscopy. *Merged images* are shown in the *right-hand column*. *Bottom*, MDCKBcl-2 cells were infected with PR8 (1.5 MOI) and processed as described for the MDCK cells. Shown are confocal images of cells labeled 8 h postinfection with anti-NP Abs (*NP*) and anti-phospho-p38MAPK Abs (*P-p38*). *Merged images* are shown in the *right-hand column*. D, *top*, MDCK cells were treated continuously with different concentrations (10–20 μM) of SB203580, SB202474, or DMSO (controls) for 1 h before and 24 h after infection (*I*) with PR8 (0.05 MOI to allow multicycle replication). Supernatant samples were collected and analyzed for infectious virions by plaque assay. Data represent the mean ± S.D. (*n = 6*) of results from three separate experiments, each performed in duplicate. *, $p < 0.05$ *versus* I + DMSO. *Bottom*, MDCK cells were transfected with siRNA against p38MAPK (*si p38*) or with scrambled siRNA (*si Scr*), and 12 h later the transfected cells were infected with a high MOI (1.5) of PR8. Eight hours postinfection, supernatant samples were collected and analyzed for infectious virions by plaque assay. Data represent the mean ± S.D. (*n = 4*) of results from two separate experiments, each performed in duplicate. *, $p < 0.05$ *versus* si Scr cells. *p.f.u.*, plaque-forming units.

with modified glycosylation of the viral hemagglutinin protein, and our group itself (6) has demonstrated the negative effect of high intracellular levels of GSH in Bcl-2$^+$ cells on the expression and maturation of hemagglutinin and other late viral proteins.

Our present findings indicate that host cell expression of Bcl-2 has a dual impact on influenza virus infection that is related to its role as a substrate of p38MAPK. The interaction of

Bcl-2 with this kinase diminishes its own ability to prevent the cell from undergoing virally induced apoptosis, but it also reduces the ability of the virus to replicate effectively. The immediate result is programmed death of infected cells and the release of a relatively low number of infective virions. In a broader context, however, virus replication and host cell responses in Bcl-2$^+$ and Bcl-2$^-$ cells are likely to reflect the net effect of parallel or contrasting signals activated by the virus, which would be determined by levels of Bcl-2 expression, p38MAPK activation, caspase-3 activation, and GSH content. It is worth noting that in complex epithelial tissues, such as those found in the lungs, intestine, and skin (49, 50), loss of Bcl-2 expression correlates with differentiation and loss of proliferative capacity. In particular, Bcl-2 is absent in the normal, well differentiated epithelial cells of human airways (11), where influenza virus replication is known to be highly productive (1), but it is expressed in metaplastic mucous cells whose number increases during situations of chronic inflammation (*e.g.* cystic fibrosis, asthma) (51). This differential Bcl-2 expression might thus be an important determinant of the balance between viral replication and p38MAPK-mediated inflammation or apoptosis in the airways. Further studies are needed to clarify these points.

It should also be recalled that the influenza virus can spread from the airways through the olfactory bulb to the brain, where it selectively targets several structures implicated in the pathogenesis of neuropsychiatric disturbances and behavioral changes (52). Both high and low pathogenicity isolates of influenza A/H5N1 virus have been recovered from the olfactory bulbs following intranasal instillation in mice and ferrets (53, 54). Neuronal cells are characterized by high expression of Bcl-2 (10) and relatively low permissiveness to influenza virus replication (6). Our current findings provide a possible explanation for this reduced permissiveness. They suggest, however, that despite limited viral replication, some degree of damage might still be provoked in the brain by the apoptotic death of

infected neurons, which is made possible in part by p38MAPK-mediated phosphorylation of Bcl-2.

Finally, highly pathogenic influenza A virus strains are known to cause hyperactivation of p38MAPK (36). It is reasonable to speculate that, during infection with a strain of this type, one might encounter higher rates of apoptosis in Bcl-2$^+$ cells together with higher rates of viral replication in Bcl-2$^-$ cells. This might represent an additional mechanism that influences the severity of infection.

The fact that a cellular kinase like p38MAPK is involved in both influenza virus replication and virally induced apoptosis has intriguing implications for the development of novel anti-influenza strategies aimed at limiting both the acute respiratory effects of influenza and its potential neurological complications.

REFERENCES

1. Fields, B. N., Knipe, D. M., and Howley, P. M. (2007) *Virology*, 3rd Ed., Vol. 2, pp. 1647–1740, Lippincott-Raven Publishers, Philadelphia
2. Cros, J. F., and Palese, P. (2003) *Virus. Res.* **95,** 3–12
3. Boulo, S., Akarsu, H., Ruigrok, R. W. H., and Baudin, F. (2007) *Virus. Res.* **124,** 12–21
4. Bui, M., Wills, E. G., Helenius, A., and Whittaker, G. R. (2000) *J. Virol.* **74,** 1781–1786
5. Pleschka, S., Wolff, T., Ehrhardt, C., Hobom, G., Planz, O., Rapp, U. R., and Ludwig, S. (2001) *Nat. Cell. Biol.* **3,** 301–305
6. Nencioni, L., Iuvara, A., Aquilano, K., Ciriolo, M. R., Cozzolino, F., Rotilio, G., Garaci, E., and Palamara, A. T. (2003) *FASEB. J.* **17,** 758–760
7. Palamara, A. T., Nencioni, L., Aquilano, K., De Chiara, G., Hernandez, L., Cozzolino, F., Ciriolo, M. R., and Garaci, E. (2005) *J. Infect. Dis.* **191,** 1719–1729
8. Wurzer, W. J., Planz, O., Ehrhardt, C., Giner, M., Silberzahn, T., Pleschka, S., and Ludwig, S. (2003) *EMBO. J.* **22,** 2717–2728
9. Shin, Y. K., Li, K., Liu, Q., Anderson, D. H., Babiuk, L. A., and Zhou, Y. (2007) *J. Virol.* **81,** 12730–12739
10. Levine, B., Huang, Q., Isaacs, J. T., Reed, J. C., Griffin, D. E., and Hardwick, J. M. (1993) *Nature* **361,** 739–742
11. Tesfaigzi, J., Hotchkiss, J. A., and Harkema, J. R. (1998) *Am. J. Respir. Cell. Mol. Biol.* **18,** 794–799
12. Reed, J. C. (1994) *J. Cell. Biol.* **124,** 1–6
13. Torcia, M., De Chiara, G., Nencioni, L., Ammendola, S., Labardi, D., Lucibello, M., Paolo Rosini, P., Marlier, L. N. J. L., Bonini, P., Dello Sbarba, P., Palamara, A. T., Nicola Zambrano, N., Russo, T., Garaci, E., and Cozzolino, F. (2001) *J. Biol. Chem.* **276,** 39027–39036
14. Rosini, P., De Chiara, G., Lucibello, M., Garaci, E., Cozzolino, F., and Torcia, M. (2000) *Biochem. Biophys. Res. Commun.* **278,** 753–759
15. De Chiara, G., Marcocci, M. E., Torcia, M., Lucibello, M., Rosini, P., Bonini, P., Higashimoto, Y., Damonte, G., Armirotti, A., Amodei, S., Palamara, A. T., Russo, T., Garaci, E., and Cozzolino, F. (2006) *J. Biol. Chem.* **281,** 21353–21361
16. Haldar, S., Jena, N., and Croce, C. M. (1995) *Proc. Natl. Acad. Sci. U. S. A.* **92,** 4507–4511
17. Olsen, C. W., Kehren, J. C., Dybdahl-Sissoko, N. R., and Hinshaw, V. S. (1996) *J. Virol.* **70,** 663–666
18. Kistner, O., Müller, K., and Scholtissek, C. (1989) *J. Gen. Virol.* **70,** 2421–2431
19. Bui, M., Myers, J. E., and Whittaker, G. R. (2002) *Virus Res.* **84,** 37–44
20. Neumann, G., Castrucci, M. R., and Kawaoka, Y. (1997) *J. Virol.* **71,** 9690–9700
21. Bullido, R., Gómez-Puertas, P., Albo, C., and Portela, A. (2000) *J. Gen. Virol.* **81,** 135–142
22. Portela, A., and Digard, P. (2002) *J. Gen. Virol.* **83,** 723–734
23. Ludwig, S., Planz, O., Pleschka, S., and Wolff, T. (2003) *Trends. Mol. Med.* **9,** 46–52
24. Ludwig, S., Pleschka, S., Planz, O., and Wolff, T. (2006) *Cell. Microbiol.* **8,** 375–386
25. Tibbles, L. A., and Woodgett, J. R. (1999) *Cell. Mol. Life. Sci.* **55,** 1230–1254
26. Pica, F., Palamara, A. T., Rossi, A., De Marco, A., Amici, C., and Santoro, M. G. (2000) *Antimicrob. Agents Chemother.* **44,** 200–204
27. Gaush, C. R., and Smith, T. F. (1968) *Applied Microbiol.* **16,** 588–594
28. Mahy, B. W. J. (1991) *Virology: A Practical Approach*, pp. 119–150, IRL Press, Oxford
29. Nicoletti, I., Migliorati, G., Pagliacci, M. C., Grignani, F., and Riccardi, C. (1991) *J. Immunol. Methods* **139,** 271–279
30. Aquilano, K., Vigilanza, P., Rotilio, G., and Ciriolo, M. R. (2006) *FASEB J.* **20,** 1683–1685
31. Blagosklonny, M. V. (2001) *Leukemia* **15,** 869–874
32. Kujime, K., Hashimoto, S., Gon, Y., Shimizu, K., and Horie, T. (2000) *J. Immunol.* **164,** 3222–3228
33. Maruoka, S., Hashimoto, S., Gon, Y., Nishitoh, H., Takeshita, I., Asai, Y., Mizumura, K., Shimizu, K., Ichijo, H., and Horie, T. (2003) *Biochem. Biophys. Res. Comm.* **307,** 870–876
34. Lee, J. C., Kassis, S., Kumar, S., Badger, A., and Adams, J. L. (1999) *Pharmacol. Ther.* **82,** 389–397
35. DeSilva, D. R., Jones, E. A., Favata, M. F., Jaffee, B. D., Magolda, R. L., Trzaskos, J. M., and Scherle P. A. (1998) *J. Immunol.* **160,** 4175–4181
36. Lee, D. C. W., Cheung, C.-Y., Low, A. H. J., Mok, C. K. P., Peiris, M., and Lau, A. S. Y. (2005) *J. Virol.* **79,** 10147–10154
37. Uchide, N., Ohyama, K., Bessoh, T., and Toyoda, H. (2007) *Intervirology* **50,** 99–107
38. Hinshaw, V. S., Olsen, C. W., Dybdahl-Sissoko, N., and Evans, D. (1994) *J. Virol.* **68,** 3667–3673
39. Galluzzi, L., Brenner, C., Morselli, E., Touat, Z., and Kroemer, G. (2008) *PLoS Pathog.* **4,** e1000018
40. O'Neill, R. E., Talon, J., and Palese, P. (1998) *EMBO J.* **17,** 288–296
41. Neumann, G., Hughes, M. T., and Kawaoka, Y. (2000) *EMBO J.* **19,** 6751–6758
42. Elton, D., Simpson-Holley, M., Archer, K., Medcalf, L., Hallam, R., McCauley, J., and Digard, P. (2001) *J. Virol.* **75,** 408–419
43. Akarsu, H., Burmeister, W. P., Petosa, C., Petit, I., Müller, C. W., Ruigrok, R. W., and Baudin, F. (2003) *EMBO J.* **22,** 4646–4655
44. Whittaker, G., and Helenius, A. (1998) *Virology* **246,** 1–23
45. Hirayama, E., Atagi, H., Hiraki, A., and Kim, J. (2004) *J. Virol.* **78,** 1263–1270
46. Garland, L. G., Bonser, R. W., and Thompson, N. T. (1987) *Trends. Pharmacol. Sci.* **8,** 334
47. Frémont, L. (2000) *Life. Sci.* **66,** 663–673
48. Zachos, G., Koffa, M., Preston, C. M., Clements, J. B., and Conner, J. (2001) *J. Virol.* **75,** 2710–2728
49. Hockenbery, D. M., Zutter, M., Hickey, W., Nahm, M., and Korsmeyer, S. J. (1991) *Proc. Natl. Acad. Sci. U. S. A.* **88,** 6961–6965
50. Gompel, A., Sabourin, J. C., Martin, A., Yaneva, H., Audouin, J., Decroix, Y., and Poitout, P. (1994) *Am. J. Pathol.* **144,** 1195–1202
51. Harris, J. F., Fischer, M. J., Hotchkiss, J. R., Monia, B. P., Randell, S. H., Harkema, J. R., and Tesfaigzi, Y. (2005) *Am. J. Respir. Crit. Care. Med.* **171,** 764–772
52. Kristensson, K. (2006) *Brain Res. Bull.* **68,** 406–413
53. Tanaka, H., Park, C.-H., Ninomiya, A., Ozaki, H., Takada, A., Umemura, T., and Kida, H. (2003) *Vet. Microbiol.* **95,** 1–13
54. Maines, T. R. (2005) *J. Virol.* **79,** 11788–11800